GSC Biological and Pharmaceutical Sciences

eISSN: 2581-3250 CODEN (USA): GBPSC2

Cross Ref DOI: 10.30574/gscbps

Journal homepage: https://gsconlinepress.com/journals/gscbps/

(RESEARCH ARTICLE)

Check for updates

# Histopathological examination of *Allolobophora calignosa* efficacy against glucocorticoid-induced osteoporosis in mice

Marwa Ahmed Abdelfattah, Ayman Saber Mohamed *, Sherif Abdelaziz Ibrahim and Sohair R. Fahmy

*Department of Zoology, Faculty of Science, Cairo University 12613, Giza, Egypt.*

GSC Biological and Pharmaceutical Sciences, 2023, 22(01), 125–133

Publication history: Received on 25 November 2022; revised on 09 January 2023; accepted on 11 January 2023

Article DOI: https://doi.org/10.30574/gscbps.2023.22.1.0499

## Abstract

Osteoporosis is a disease characterized by low bone mass, deterioration of bone tissue, and disruption of bone microarchitecture: it can lead to compromised bone strength and increased risk of fractures. Secondary osteoporosis is mostly glucocorticoid-induced osteoporosis (GIOP). According to traditional Chinese medicine, the kidney influences bone, and bone loss are associated with kidney and liver inadequacies. We tested *Allolobophora caliginosa* extract (EE) and *Allolobophora caliginosa* coelomic fluid (CF) for anti-osteoporotic activity against GIOP. 28 male mice were separated randomly into two groups; the control received distilled water, and the second group received 1 mg/kg dexamethasone daily for 28 days. The second group was divided randomly into three groups. The first OP subgroup received distilled water orally every other day for 28 days. The other two OP subgroups received EE (45 mg/kg body weight) and CF (20 mg/kg) orally for 28 days. EE and CF preserved cortical and trabecular bone loss, decreased bone marrow space, and enhanced chondrocyte production. EE and CF maintained hepatic necrosis in the liver and decreased renal degeneration in the kidney caused by GIOP. In this study, Histological images showed that EE at 45 mg/kg was highly effective as an anti-osteoporotic against GIOP, while CF at 20 mg/kg was moderately effective.

**Keywords:** Glucocorticoids; Osteoporosis; Earthworm; Antiosteoporosis

## 1. Introduction

Bone is a valuable, living tissue that alters all the time. This process aims to replace the old micro-damaged bones with new, stronger ones (1). This procedure is done with groups of osteoclasts, which break down bone, and osteoblasts, which build up the bone (2).

Osteoporosis (OP) is characterized by a loss of bone mass and deterioration of bone structure (3). This causes bones to be thin, directly affecting cortical porosity, bone fragility, and the risk of breaking a bone (4).

Many factors contribute to the risk of osteoporosis and fracture associated with aging; hormonal factors, limited physical activity, a lack of physical activity, a lack of calcium or vitamin D, pharmacological therapy such as glucocorticoids (GCs), and inherited features (5).

GCs are widely utilized to treat various systemic disorders as they are important anti-inflammatory and immunosuppressive agents (6). In contrast, long-term use of GCs promotes bone loss and osteoporosis by killing osteocytes and osteoblasts (7) and increases reactive species generation, producing skewed bone remodeling and an imbalance between osteoclasts and osteoblasts (8). Furthermore, GCs indirectly affect bone by lowering gastrointestinal calcium absorption and increasing renal calcium loss, altering calcium homeostasis.

* Corresponding author: Ayman Saber Mohamed

The most prevalent type of secondary osteoporosis is glucocorticoid-induced osteoporosis (GIOP) (9,10). Compared to short-acting medications like methylprednisolone, synthetic long-acting GC dexamethasone (DEX) produces more serious side effects (11).

Bisphosphonates, such as alendronate, are the most regularly used and effective anti-osteoporosis medications. However, bisphosphonates increase the likelihood of developing osteonecrosis of the jaw (12,13). Teriparatide (a recombinant PTH) has also been proven to lower fracture risk, but it has a very high cost and an inconvenient way of administration (14). While denosumab successfully prevents bone loss and increases bone mass in glucocorticoid-treated patients, there is a concern about temporary bone loss and increased fracture risk when the drug is stopped (15).

As a result, antiosteoporosis induced by natural materials may be less toxic. In the treatment, natural products have been demonstrated to be very efficacious (3). The earthworm has proven a competitive medicinal importance in treating various diseases due to its biological activities. The body cavity of earthworms comprises a coelomic fluid, which has anti-inflammatory capabilities (16). Extract of earthworm (*Pheretima aspergillum*) increases osteoblast activity and inhibits the generation of osteoclasts (17).

## 2. Material and methods

### 2.1. Collection of earthworms

Earthworms of the species *Allolobophora caliginosa* were picked from commercial vermiculture in the Giza Governorate and kept in small containers with the decomposed organic matter until they were used in a study.

### 2.2. Preparation of earthworm extract (EE)

According to Sucindra Dewi *et al*.(18), EE was extracted with some modifications. Earthworms were starving for 24 hours to get rid of all the mud in their guts. After being cleaned, worms were cut into small pieces, smoothed, and transferred into a glass beaker containing ethanol (80%). Then, samples were centrifuged for 10 minutes at 3000 rpm. Finally, the supernatant was collected and evaporated in a water bath and oven for complete dryness.

### 2.3. Preparation of earthworm coelomic fluid (CF)

The thermal method proved to be the most productive in extracting coelomic fluid (19). After placing the earthworms in a dry petri dish on a hot plate at temperatures between 55 and 60 ° C, the fluid was freeze-dried.

### 2.4. Animals

Adult male BALB/c mice (*Mus musculus*) were used in all experiments. Animals with an average body weight of 33-35 g were purchased from the National Research Center (NRC, Cairo, Egypt), housed in polypropylene cages (6 animals/cage) at a temperature of (22-25) °C under 12:12 h day/night cycles, and supplied with a standard laboratory diet and water *ad libitum*. All experimental techniques were conducted by international animal care standards and used in laboratories.

### 2.5. Acute Toxicity test (LD50)

$LD_{50}$ of CF and EE was determined according to Chinedu *et al.*(20).The mice were starved overnight and then divided into four groups (n=2), one for CF and one for EE (2 mice per dose). Doses of 10, 100, 300, and 600 mg/kg were intraperitoneally injected with EE and CF. After intraperitoneal administration, the animals were monitored for 1 hour, then 10 minutes every 2 hours for the next 24 hours. The animals were observed for any changes in behavior, such as paw licking, weariness, semi-solid feces, salivation, writhing or death. EE dose was $=\frac{M0+M1}{2} = \frac{300+600}{2} = 45\ mg/kg$, and CF dose was = $\frac{100+300}{2} = 20\ mg/kg$ , where M0 is the greatest dose that did not cause mortality and M1 is the lowest dose that did cause mortality.

### 2.6. Experimental design

All animal procedures were evaluated and approved by the Ethical committee Office of the Faculty of

Sciences, Cairo University, Egypt (Registration number: CU/I/F/73/20).

Osteoporosis was induced in mice by subcutaneous injection of 1 mg/kg dexamethasone five times per week for 30 days (21). The control group was injected with 0.9% saline. Mice were randomly separated into four groups (n=6 per group) and concurrently treated as follows:

- Group I Control: Animals were subjected to intraperitoneal injection with distilled water day after day for 30 days.
- Group II glucocorticoid-induced osteoporosis model (OP): Animals were subjected to intraperitoneal injection with distilled water day after day for 30 days.
- Group III OP and CF: Animals were subjected to intraperitoneal injection with CF (20 mg/kg body weight) day after day for 30 days.
- Group IV OP and EE: Animals were subjected to intraperitoneal injection with EE (45 mg/kg body weight) day after day for 30 days.

At the end of the experiment, animals were anesthetized by cervical dislocation. femur bone, kidney, and liver were dissected for histological examination.

### 2.7. Histopathological examination

Liver and kidney tissues were fixed in 10% formal saline, embedded in paraffin, and sectioned. Then, the sections were stained with hematoxylin and eosin (H&E) for histological examination using a light microscope (OPTRCH, Germany).

The femurs were first fixed for two days in 10% neutral buffered formalin, followed by two weeks of decalcification in 10% EDTA (pH 7.4), and finally, paraffin embedding. The samples were cut into 5-μm thick slices along the coronal plane. The sections were stained with hematoxylin and eosin (H&E) to examine the histological characteristics of the trabecular and cortical bones under a light microscope (OPTRCH, Germany).

## 3. Results

### 3.1. Acute toxicity study

*3.1.1. Histopathology of CF and EE doses on liver and kidney*

Microscopic examination of CF-1, doses 10 mg/kg revealed normal liver parenchyma (Fig. 1a). Meanwhile, kidney sections revealed mild degenerative changes in the lining epithelium of renal tubules represented by vacuolation (Fig. 1e). Liver sections of CF-2, dose 100 mg/kg showed focal aggregations of mononuclear inflammatory cells within the hepatic parenchyma (Fig. 1b). Focal areas of hepatocytes necrosis were also detected. The examined kidney sections showed renal tubular degeneration represented by vacuolation and swelling that resulted in complete obliteration of their lumen (Fig. 1f). Likewise, liver sections from CF-3 dose 300 mg/kg showed focal hepatocellular necrosis with mononuclear inflammatory cells infiltration. The portal areas exhibited inflammatory cells infiltrations (Fig. 1c). In comparison, kidney sections showed mild renal tubular degeneration (Fig. 1g). CF-4 dose 600 mg/kg, the examined liver sections exhibited hepatocellular necrosis, hemorrhage, and mononuclear inflammatory cells infiltration (Fig. 1d). Kidney sections of group CF-4 showed renal tubular degeneration and necrosis with marked swelling in the lining epithelium that resulted in narrowing or complete obliteration of the renal tubular lumen (Fig. 1h).

Microscopic examination of EE-1 group of dose 10 mg/kg revealed liver samples of normal hepatic parenchyma (Fig. 2a) same in kidney sections that apparently revealed normal renal cortex and medulla (Fig. 2e). Liver sections from EE-2 group of dose 100 mg/kg showed small multifocal aggregations of mononuclear inflammatory cells scattered within the hepatic parenchyma with activation of Kupffer cells (Fig. 2b), meanwhile kidney sections showed degenerative changes in the renal tubular epithelium represented by marked vacuolation and cellular swelling leading to narrowing of tubular lumen or even complete obliteration (Fig. 2f). EE-3 group of dose 300 mg/kg exhibited congestion with focal or diffuse mononuclear inflammatory with infiltrations (Fig. 2c) while kidney sections showed some renal tubules suffered from degeneration and necrosis with existence of interstitial nephritis manifested by the presence of mononuclear inflammatory cells in the interstitial tissue (Fig. 2g). Mild fibroplasia was also noticed concerning EE-4 group of dose 600 mg/kg where, the examined liver sections showed focal areas of hepatocellular necrosis with inflammatory cells infiltration (Fig. 2d). Renal tubular degeneration and necrosis were the most frequently detected lesion in the examined kidney sections from EE-4 group (Fig. 2h). In addition to mild interstitial nephritis.

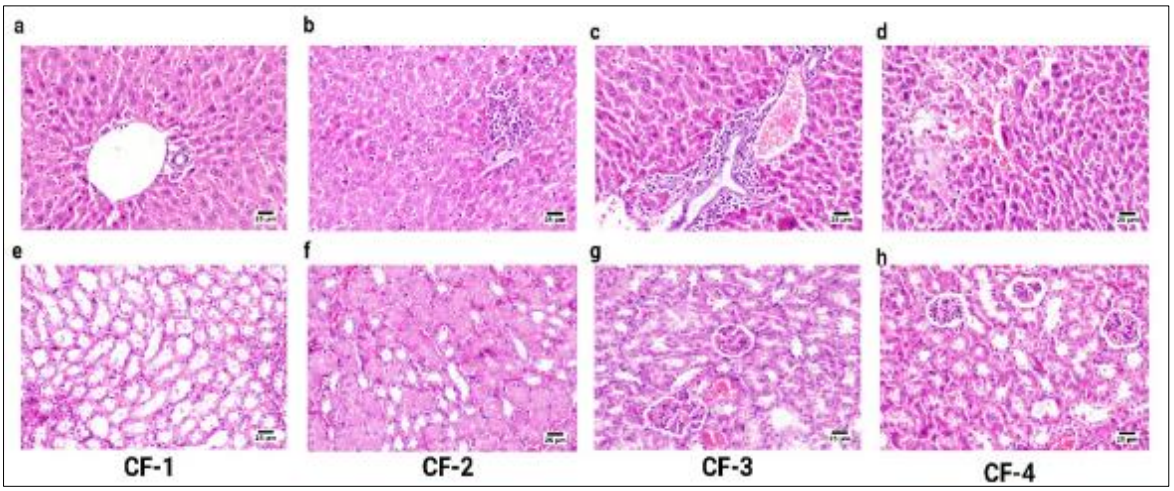


**Figure 1** Sections of the liver and kidney with different doses of earthworm coelomic fluid (CF), a. liver section treated with CF-1 of Dose 10 mg/kg, showing apparently normal liver parenchyma (H&E). b. liver section treated with CF-2 of Dose 100 mg/kg, showing a focal area of hepatocellular necrosis with inflammatory cells infiltration (H&E). c. liver section treated with CF-3 of Dose 300 mg/kg showing portal infiltration with mononuclear inflammatory cells (arrow) (H&E). d. liver sections treated with CF-4 of Dose 600 mg/kg, showing areas of hemorrhage with loss of hepatic parenchyma (H&E). e. kidney section treated with CF-1 of Dose 10 mg/kg, showing mild vacuolation in the lining epithelium of renal tubules (H&E). f. kidney section treated with CF-2 of Dose 100 mg/kg, showing swelling of the renal tubular epithelium (H&E). g. kidney section treated with CF-3 of Dose 300 mg/kg, showing necrosis in the renal tubular epithelium (H&E). h. kidney section treated with CF-4 of Dose 600 mg/kg, renal tubular degeneration, and necrosis (H&E).

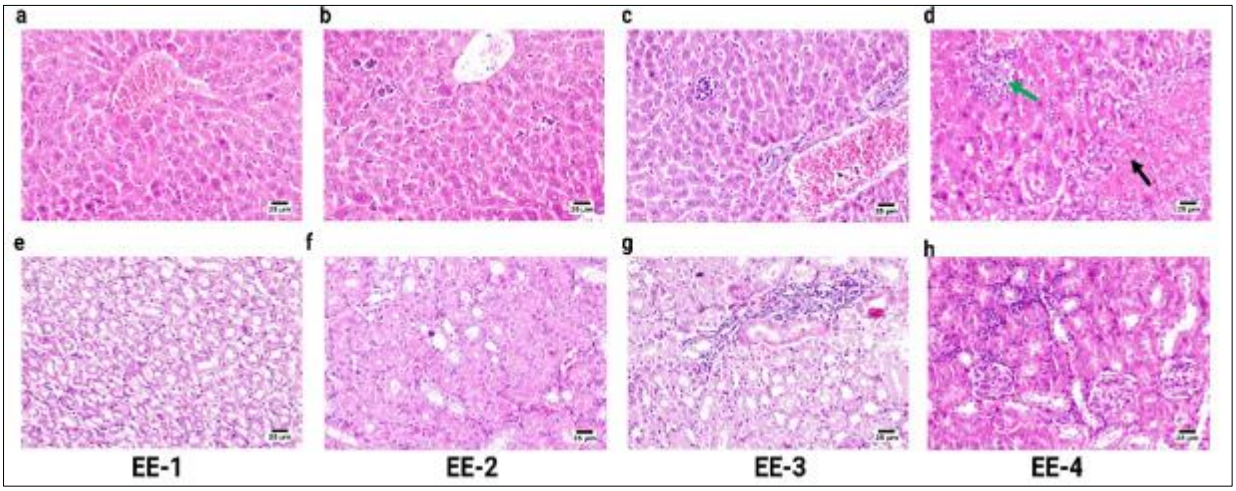


**Figure 2** Sections of the liver and kidney with different doses of earthworm extract (EE). a. liver section treated with EE-1 of Dose 10 mg/kg, showing normal centrilobular hepatocytes (H&E). b. liver section treated with EE-2 of Dose 100 mg/kg, showing small multifocal aggregation of mononuclear inflammatory cells (H&E). c. liver section treated with EE-3 of Dose 300 mg/kg, showing focal mononuclear inflammatory cells infiltration with congested portal blood vessel (H&E). d. liver section treated with EE-4 of Dose 600 mg/kg, showing portal mononuclear inflammatory cells infiltration (black arrow) and focal hepatocellular necrosis with inflammatory cells infiltration (green arrow) (H&E). e. kidney section treated with EE-1 of Dose 10 mg/kg, showing apparently normal renal medulla (H&E). f. kidney section treated with EE-2 of Dose 100 mg/kg, showing degeneration and necrosis in the renal tubular epithelium (H&E). g. kidney section treated with EE-3 of Dose 300 mg/kg, showing mononuclear inflammatory cells infiltration with mild fibroplasia, note vacuolation of the renal tubular epithelium (H&E). h. kidney section treated with EE-4 of Dose 600 mg/kg, showing mononuclear inflammatory cells infiltration with renal tubular necrosis (H&E)

### 3.2. Histopathology of bone

A microscopic inspection of bone sections from the control group revealed thick, normal-appearing trabecular bone with chondrocytes (Fig. 3a). In the OP group, the bone trabeculae were defective and short, resulting in large marrow gaps (Fig. 3b). The EE group showed seemingly normal bone trabeculae and a histologically normal shaft (Fig. 3c). In the CF group, the examined sections revealed a little reduction in the thickness of the bony trabeculae at the bone's head with an increasing number of chondrocytes compared to the normal (Fig. 3d).

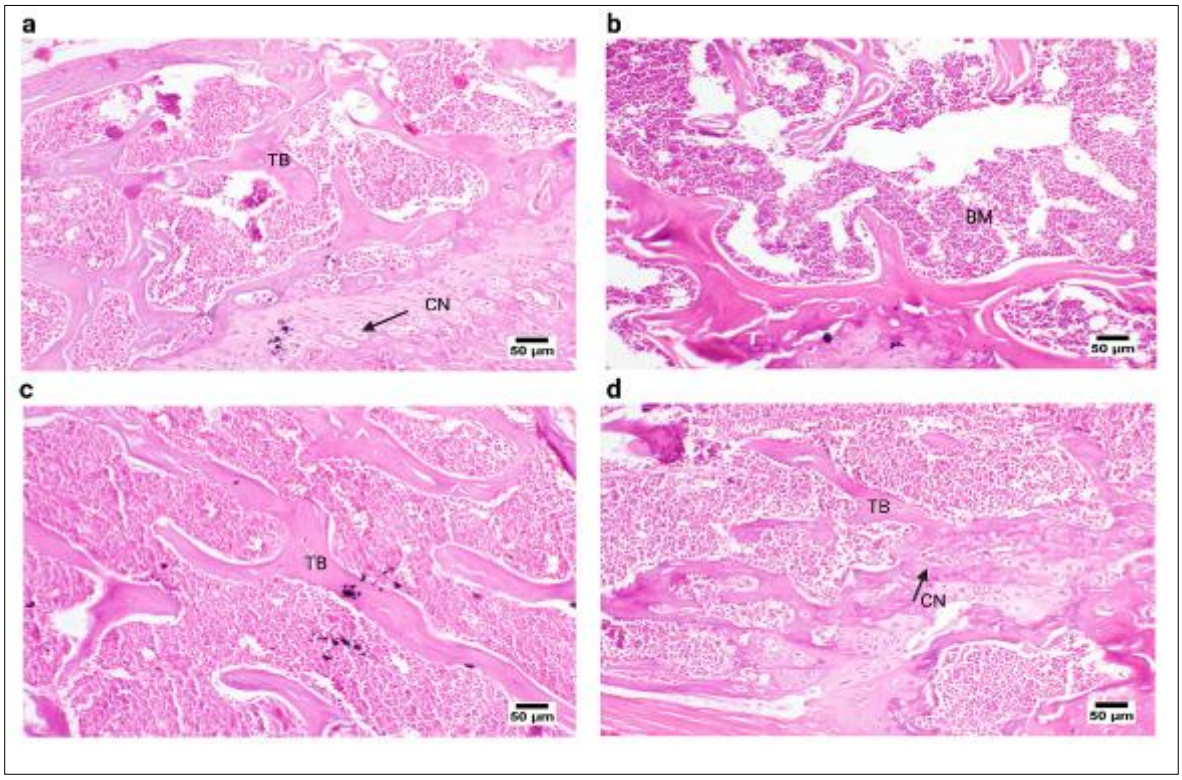


**Figure 3** The histopathological examination of the femur bone. TB: trabecular bone, CN: chondrocytes, BM: bone marrow. a. control group showing normal trabeculae (TB) with normal chondrocytes (CN), (H&E). b. OP group showing short and incomplete bone trabeculae with defective mineralization and vacuolation of bone marrow (BM), (H&E). c. EE group showing apparently normal bone trabeculae (H&E). d. CF group showing normal bone trabeculae with enhancement in number of chondrocytes

### 3.3. Histopathology of the liver

Microscopic examination of liver sections from the control group (Fig. 4a) revealed a normal histological structure of hepatic parenchyma; both portal and centrilobular hepatocytes are normal. OP group (Fig. 4b) showed multifocal areas of hepatocellular necrosis with inflammatory cell infiltration. The hepatic sinusoids were dilated with atrophied hepatic cords. Portal infiltration with mononuclear inflammatory cells was also noticed. Severely congested hepatic vasculature was detected in many sections. Concerning the EE group (Fig. 4c), the examined liver sections were normal except for a few severely affected individuals that exhibited mild multifocal mononuclear inflammatory cell aggregations within the hepatic parenchyma. Some sections showed mild portal fibroplasia mixed with mononuclear inflammatory cell infiltration. The liver of the CF group (Fig. 4d) showed marked histopathological changes; multifocal areas of mononuclear inflammatory cell aggregations were noticed within the hepatic parenchyma. Focal hepatocellular necrosis was frequently observed with mononuclear inflammatory cell infiltration.

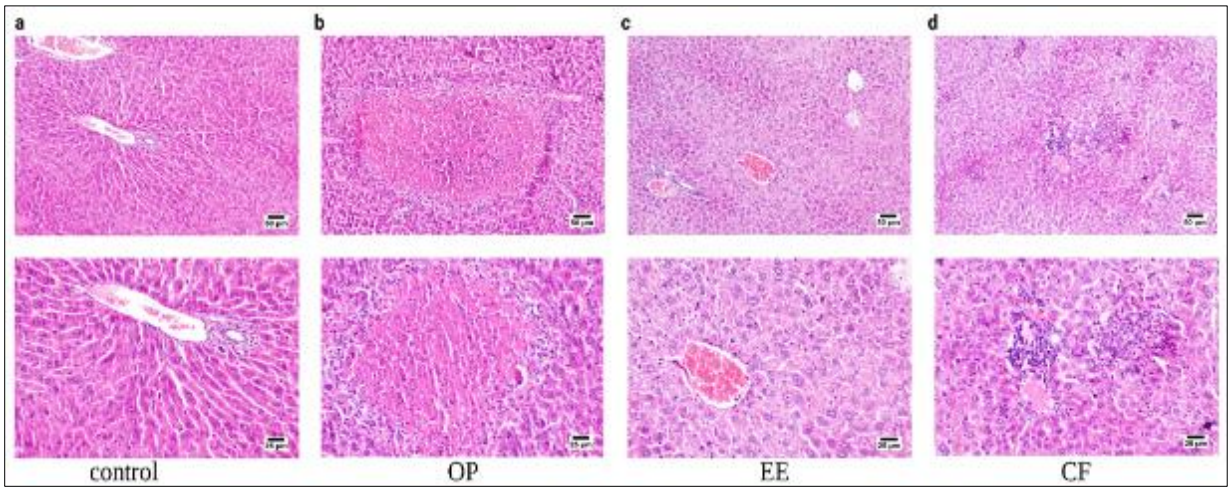


**Figure 4 a** Photomicrograph of the liver, Control group, showing the normal portal area (H&E). b. Photomicrograph of the liver, OP group showing an area of hepatocellular necrosis with inflammatory cell infiltration (H&E). c. Photomicrograph of the liver, EE-group showing apparently normal hepatic parenchyma (H&E). d. Photomicrograph of the liver, CF-group showing multifocal aggregations of mononuclear inflammatory cells (arrows) (H&E)

### 3.4. Histopathology of kidney

Histopathological examination of kidney tissue from the control group (Fig. 5a) revealed the absence of any histopathological alterations in both the renal cortex and medulla. Glomeruli and tubules were histologically normal. On the contrary, the OP group (Fig. 5b) showed marked renal damage, renal vasculature was severely congested, and the renal cortex showed focal to diffuse infiltrations with mononuclear inflammatory cells. Renal tubules in both cortex and medulla showed degeneration and cellular swelling aggravated in some sections into complete necrosis of renal tubules. Kidney sections from the EE group (Fig. 5c) showed a normal renal cortex in almost all examined sections except for a few sections that exhibited the presence of small focal aggregation of mononuclear inflammatory cells. The renal medulla from this group was also normal, with mild vacuolation in the renal tubular epithelium. Regarding CF-group (Fig. 5d), minor histopathological alterations were reported in the examined kidney sections, represented by mild vascular congestion and mild cystic dilatation in the renal tubules.

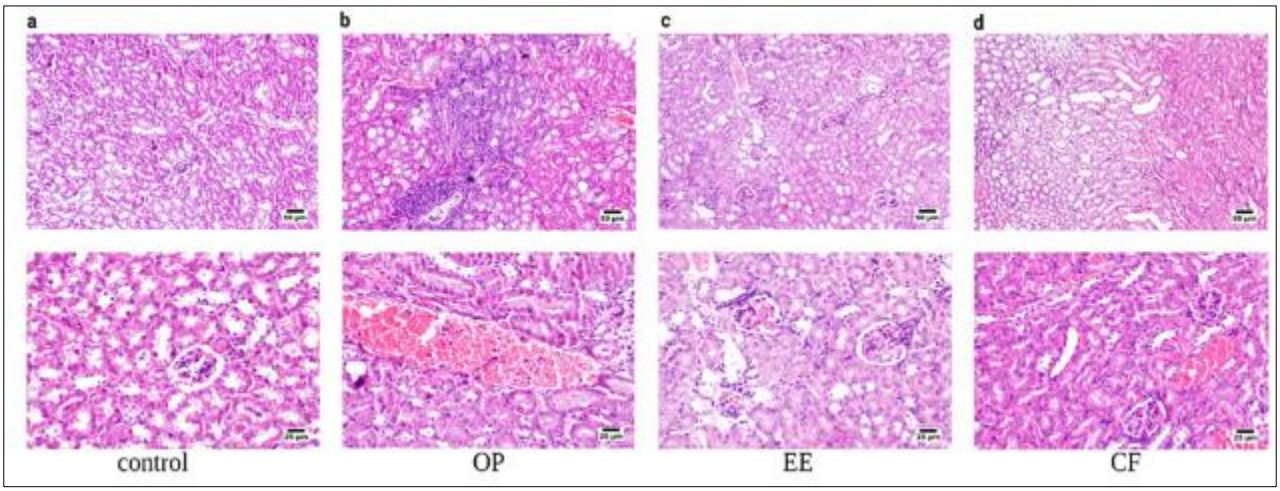


**Figure 5 a** Photomicrograph of Kidney, Control group showing normal renal cortex (H&E). b. Photomicrograph of Kidney, Model group showing severely congested blood vessel in the renal cortex (H&E). c. Photomicrograph of Kidney, Extract group higher magnification showing apparently normal renal cortex with a congested glomerular capillary tuft (H&E). d. Photomicrograph of Kidney, CF- group showing few cystically dilated tubules in the renal medulla (H&E)

## 4. Discussion

GIOP is the most prevalent iatrogenic cause of secondary osteoporosis. It poses a major risk to the general public's health. In the present investigation, it was revealed that EE and CF could suppress GIOP in DEX-treated mice.

In the current study, compared to the controls, OP mice exhibited significant resorption and reduction in the thickness of bony trabeculae, as well as shrinkage of cartilage cores and a decrease in the number of chondrocytes prompting vacuolation of the bone marrow spaces. Similar studies by Wei *et al*. (22) discovered that the femoral cancellous bone exhibited substantial bone resorption, as shown by significant thinning and irregularity of the bone trabeculae. Analysis shows that the histopathology of normal and osteoporotic bones reported that patients with osteoporosis had cortical effacement and a decrease in the density and integrity of trabecular bone (23). According to reports, the pathogenesis of GIOP generates a free radical that affects the compromise between bone growth and resorption (24). GCs alter calcium absorption, affect bone mineral density, and increase osteoblast apoptosis which is associated with increased bone resorption (25).

According to traditional Chinese medicine, the kidney influences bone, and bone loss are associated with kidney and liver inadequacies (26). In the OP group, liver sections have shown hepatocellular necrosis with inflammatory cell infiltration compared to the control group. It was reported that GCs inhibit the oxidation of fatty acids leading to hepatocellular deterioration (27). In addition to the kidney, sections showed significant renal damage, renal vasculature was severely congested, and the renal cortex showed focal to diffuse infiltrations with mononuclear inflammatory cells. Inconsistent with a previous study by Cesini *et al.* (28) reported that osteoporosis patients frequently experience an age-related impairment in renal function via promoting the development of vascular calcifications.

Bone sections of OP mice treated with EE at a Dose of 45mg/kg were found to be effective and highly significant, with a marked increase in the thickness of the cortical bone that prevented cortically as well as trabecular bone loss. In contrast, CF Dose (20 mg/kg) was found to be moderately significant, with a slight increase in the thickness of the cortical bone that prevented cortically as well as trabecular bone loss compared to that in OP. This could imply that EE and CF considerably influence osteoporotic bone. Our findings were consistent with prior research, which indicated that glycolipid protein extract from earthworms protected against free radical toxicity and encouraged the proliferation of human fibroblasts and epithelial cells (29).

In addition, kidney and liver sections treated with EE and CF showed improvement in the histopathological examination. Phenolic compounds present in EE and CF may be responsible for the antioxidant activity that protects the kidney and liver from oxidative stress induced by GIOP. Inconsistent with the current study, it was reported that the earthworm extract prevents the formation of reactive oxygen groups, preventing damage to the hepatic cells and modulating the genes responsible for synthesizing antioxidant enzymes (30).

## 5. Conclusion

The findings of this study demonstrate that EE and CF have strong anti-osteoporotic against the OP-treated mice. EE and CF can therefore counteract bone deterioration induced by glucocorticoids.

## Compliance with ethical standards

### *Acknowledgments*

We are very thankful to the Science, Technology, and Innovation Funding Authority of Egypt (STDF) for the funded provided by them (Post Graduate Support Grant (PGSG)) ID#45079.

### *Disclosure of conflict of interest*

The authors declare that there is no conflict of interest.

### *Statement of ethical approval*

Experimental protocols and procedures were approved by Cairo University Institutional Animal Care and Use Committee (CU-IACUC) (Egypt) (CU/I/F/73/20). Animal handling and experimentation complied with the ethical standards established by the Egyptian animal welfare laws and regulations and were performed in line with the Guide for the Care and Use of Laboratory Animals, 8th edition.

## References


[1] Tu KN, Lie JD, Wan CK, Cameron M, Austel AG, Nguyen JK, Van K, Hyun D. Osteoporosis: a review of treatment options. Pharmacy and Therapeutics. 2018 Feb;43(2):92.

[2] Li X, Liu D, Li J, Yang S, Xu J, Yokota H, et al. Wnt3a involved in the mechanical loading on improvement of bone remodeling and angiogenesis in a postmenopausal osteoporosis mouse model. FASEB J. 2019 Aug;33(8):8913-8924.

[3] An J, Yang H, Zhang Q, Liu C, Zhao J, Zhang L, et al. Natural products for treatment of osteoporosis: The effects and mechanisms on promoting osteoblast-mediated bone formation. Life Sci. 2016 Feb 15; 147:46–58.

[4] Pacheco-Costa R, Kadakia JR, Atkinson EG, Wallace JM, Plotkin LI, Reginato RD. Connexin37 deficiency alters organic bone matrix, cortical bone geometry, and increases Wnt/β-catenin signaling. Bone. 2017 Apr 1; 97:105–13.

[5] Peng CH, Lin WY, Li CY, Dharini KK, Chang CY, Hong JT, et al. Gu Sui Bu (Drynaria fortunei J. Sm.) antagonizes glucocorticoid-induced mineralization reduction in zebrafish larvae by modulating the activity of osteoblasts and osteoclasts. J Ethnopharmacol. 2022 Oct 28;297:115565.

[6] Bazsó A, Szappanos Á, Patócs A, Poór G, Shoenfeld Y, Kiss E. The importance of glucocorticoid receptors in systemic lupus erythaematosus. A systematic review. Autoimmun Rev. 2015 Apr 1;14(4):349–51.

[7] Krüger BT, Steppe L, Vettorazzi S, Haffner-Luntzer M, Lee S, Dorn AK, Ignatius A, Tuckermann J, Ahmad M. Inhibition of Cdk5 Ameliorates Skeletal Bone Loss in Glucocorticoid-Treated Mice. Biomedicines. 2022 Feb 8;10(2):404.

[8] Maulana R, Helms-Lorenz M, Irnidayanti Y, van de Grift W. Autonomous motivation in the Indonesian classroom: Relationship with teacher support through the lens of self-determination theory. The Asia-Pacific Education Researcher. 2016 Jun;25(3):441-51.

[9] Gu G, Hou D, Jiao G, Wu W, Zhou H, Wang H, Chen Y. Ortho-silicic Acid Plays a Protective Role in Glucocorticoid-Induced Osteoporosis via the Akt/Bad Signal Pathway In Vitro and In Vivo. Biological Trace Element Research. 2022 Mar 21:1-3.

[10] Maricic M. Update on Glucocorticoid-Induced Osteoporosis. Rheum Dis Clin North Am. 2011 Aug 1;37(3):415–31.

[11] Tao SC, Yuan T, Rui BY, Zhu ZZ, Guo SC, Zhang CQ. Exosomes derived from human platelet-rich plasma prevent apoptosis induced by glucocorticoid-associated endoplasmic reticulum stress in rat osteonecrosis of the femoral head via the Akt/Bad/Bcl-2 signal pathway. Theranostics. 2017;7(3):733.

[12] Fraser LA, Adachi JD. Glucocorticoid-induced osteoporosis: treatment update and review. Therapeutic advances in musculoskeletal disease. 2009 Dec;1(2):71-85.

[13] Saito Y, Nakamura S, Chinen N, Shimazawa M, Hara H. Effects of anti-osteoporosis drugs against dexamethasone-induced osteoporosis-like phenotype using a zebrafish scale-regeneration model. J Pharmacol Sci. 2020 Jun 1;143(2):117–21.

[14] Hsu E, Nanes M. Advances in treatment of glucocorticoid-induced osteoporosis. Current opinion in endocrinology, diabetes, and obesity. 2017 Dec;24(6):411.

[15] Cummings SR, Ferrari S, Eastell R, Gilchrist N, Jensen JEB, McClung M, et al. Vertebral Fractures After Discontinuation of Denosumab: A Post Hoc Analysis of the Randomized Placebo-Controlled FREEDOM Trial and Its Extension. J Bone Miner Res. 2018 Feb 1;33(2):190–8.

[16] Mustafa RG, Saiqa A, Domínguez J, Jamil M, Manzoor S, Wazir S, Shaheen B, Parveen A, Khan R, Ali S, Ali NM. Therapeutic Values of Earthworm Species Extract from Azad Kashmir as Anticoagulant, Antibacterial, and Antioxidant Agents. Canadian Journal of Infectious Diseases and Medical Microbiology. 2022 Feb 7;2022.

[17] Fu YT, Chen KY, Chen YS, Yao CH. Earthworm (Pheretima aspergillum) extract stimulates osteoblast activity and inhibits osteoclast differentiation. BMC Complement Altern Med. 2014 Nov 11;14(1).

[18] Sucindra Dewi NW, Nova Mahendra A, Kencana Putra GW, Jawi IM, Made Sukrama D, Kartini NL. Ethanolic extract of the powder of red earthworm (Lumbricus rubellus) obtained from several organic farmlands in Bali, Indonesia: Analysis of total phenolic content and antioxidant capacity. Bali Med J . 2017;3.

[19] Permana S, Putri Fityanti R, Norahmawati E, Iskandar A, Anggraini Mulyadi ED, Tri Endharti A. Coelomic Fluid of Eisenia fetida Ameliorates Cetuximab to Reduce K-Ras and Vimentin Expression through Promoting RUNX3 in an AOM/DSS-Induced Colitis Associated Colon Cancer. Evidence-based Complement Altern Med. 020 Jul 19;2020:9418520.

[20] Chinedu E, Arome D, Ameh FS. A new method for determining acute toxicity in animal models. Toxicol Int. 2013 Sep;20(3):224–6.

[21] Shi J, Wang L, Zhang H, Jie Q, Li X, Shi Q, et al. Glucocorticoids: Dose-related effects on osteoclast formation and function via reactive oxygen species and autophagy. Bone. 2015 Oct 1;79:222–32.

[22] Wei J, Wang J, Gong Y, Zeng R. Effectiveness of combined salmon calcitonin and aspirin therapy for osteoporosis in ovariectomized rats. Molecular medicine reports. 2015 Aug 1;12(2):1717-26.

[23] Li R, Gong Z, Yu Y, Niu R, Bian S, Sun Z. Alleviative effects of exercise on bone remodeling in fluorosis mice. Biological Trace Element Research. 2022 Mar;200(3):1248-61.

[24] Saleh SR, Ghareeb DA, Masoud AA, Sheta E, Nabil M, Masoud IM, et al. Phoenix dactilyfera L Pits Extract Restored Bone Homeostasis in Glucocorticoid-Induced Osteoporotic Animal Model through the Antioxidant Effect and Wnt5a Non-Canonical Signaling. Antioxidants. 2022;11(3):1–28.

[25] Xi L, Song Y, Wu W, Qu Z, Wen J, Liao B, Tao R, Ge J, Fang D. Investigation of bone matrix composition, architecture and mechanical properties reflect structure-function relationship of cortical bone in glucocorticoid induced osteoporosis. Bone. 2020 Jul 1;136:115334.

[26] Xia T, Dong X, Jiang Y, Lin L, Dong Z, Shen Y, et al. Metabolomics profiling reveals Rehmanniae radix preparata extract protects against glucocorticoid-induced osteoporosis mainly via intervening steroid hormone biosynthesis. Molecules. 2019;24(2):1–16.

[27] Rahimi L, Rajpal A, Ismail-beigi F. Glucocorticoid-Induced Fatty Liver Disease Major Pathways Contributing to. Diabetes, Metab Syndr Obes Targets Ther. 2020;1133–45.

[28] Cesini J, Cheriet S, Breuil V, Lafage-Proust MH. Osteoporosis: chronic kidney disease in rheumatology practice. Joint Bone Spine. 2012 Oct 1;79:S104-9.

[29] Grdiša M, Popović M, Hrženjak T. Stimulation of growth factor synthesis in skin wounds using tissue extract (G-90) from the earthworm Eissenia foetida. Cell Biochemistry and Function: Cellular biochemistry and its modulation by active agents or disease. 2004 Nov;22(6):373-8.

[30] Jamshidzadeh A, Heidari R, Golzar T, Derakhshanfar A. Effect of eisenia foetida extract against cisplatin-induced kidney injury in rats. J Diet Suppl. 2016;13(5):551–9